Proceedings of the 14th International Conference on Environmental Remediation and Radioactive Waste Management
ICEM2011
September 25-29, 2011, Reims, France

wP – 59196

MODELING APPROACHES FOR EVALUATING THE EFFECTS OF HETEROGENEITY ON TWO-PHASE FLOW ASSOCIATED WITH THE MIGRATION OF WASTE-GENERATED GAS FROM SF/HLW- AND L/ILW REPOSITORIES IN LOW-PERMEABILITY FORMATIONS

A. Papafotiou
Intera Inc. Swiss Branch
Ennetbaden, Switzerland

R. Senger
Intera Inc. Swiss Branch
Ennetbaden, Switzerland

A. Alcolea
TK-Konsult
Zürich, Switzerland

G.W. Lanyon
Fracture Systems Ltd.
St. Ives, United Kingdom

J. Ewing
Intera Inc. Swiss Branch
Ennetbaden, Switzerland

ABSTRACT

Different low-permeability formations are considered as potential host rocks for Low / Intermediate Level waste (L/ILW) and spent fuel / high-level / long-lived intermediate-level waste (SF/HLW/ILW) in Switzerland. As part of a generic site evaluation process, emphasis is on the assessment of Mesozoic limestones, marls and claystones in six potential siting areas in Northern and Central Switzerland. An important aspect in the site evaluation process is the characterization of the low-permeability formations in terms of spatial variability of the relevant transport properties (porosity, permeability, clay content), as they may affect the migration of waste-generated gas from L/ILW and SF/HLW/ILW repositories.

Numerical modeling studies are presented, aimed at quantifying the impact of spatial variability of rock properties on gas release through the host rock on a deca- to hectometer scale. For this purpose, 2D models of an emplacement tunnel embedded in a low-permeability host rock are developed for both a sequence of limestones and marls with distinct lithological variability (Effingen Beds) and a claystone of moderate spatial variability (Opalinus Clay). For the Effingen Beds, a composite geological model is implemented, comprising stochastic representations of the different facies and the fracture systems. The facies model displays spatial variations in clay content, porosity and permeability within the different facies. The fracture model accounts for the hydraulic effects associated with the faults and fracture systems in the siting area under consideration. For the Opalinus Clay the available geostatistical information (experimental variograms of clay content, porosity, hydraulic conductivity) is used to generate a stochastic facies model based on a log-normal permeability distribution. A separate fracture network model is not established for the Opalinus Clay. A generic gas source-term is assigned to the emplacement tunnel and hydrostatic pressures are initially assumed for the host-rock domain. The comparison of the simulations with different permeability realizations indicates that the heterogeneity of the host rock introduces strong differences in the propagation of the gas pressure perturbation, resulting in significant variations in the lateral propagation of the gas front in the host rock and the gas pressure build-up in the emplacement tunnels. Despite these differences, the calculated peak pressures in the disposal cavern and gas breakthrough along the upper model boundary are similar for multiple realizations, which compare well with the simulated results for a homogeneous model with equivalent averaged properties.

INTRODUCTION

In this study, two different low-permeability formations are considered as potential host rocks for the disposal of L/ILW and SF/HLW/ILW in deep geological repositories, namely the Effingen Beds and the Opalinus Clay in Northern Switzerland.

Significant amounts of gas are generated in the repositories due to corrosion and degradation of the waste packages. Hence a demonstration is required that despite the low permeability of the host rocks the gas can escape from the backfilled underground structures without compromising the long-term safety of the engineered and geological barriers. For this purpose a generic modeling study was initiated, aimed at simulating, both for a L/ILW repository in the Effingen Beds and a SF/HLW/ILW repository in the Opalinus Clay formation, the release of gas from the backfilled emplacement tunnels through the host rock to the adjacent aquifer systems. Numerical models were elaborated, representing the two host rock formations in terms of stochastic distributions of porosity and permeability (Figure 1).

The Opalinus Clay is part of a thick Mesozoic - Tertiary sedimentary sequence in the Molasse Basin of Northern Switzerland. Lithologically, it is classified as a moderately over-consolidated claystone that has been formed by a complex burial and compaction history; in late Tertiary the Opalinus Clay reached its greatest burial depth of about 1700 m below the surface in the area of interest (present depth ranging from 400 – 900 m in the area of interest). In the selected model domain (Figure 1a), the Opalinus Clay reveals uniform thickness of around 120 m over a distance of several kilometres, dipping gently to the south-east, and is affected by faulting only at the eastern boundary. The formation is characterized by a moderate variability in clay content (range: 30 – 70%), hydraulic conductivities typically ranging between 10^{-13} – 10^{-14} m/s and porosities between 7 and 14%.

The Effingen Beds are characterized by as many as six different facies with different mineral assemblages, including an interbedded sequence of limestone layers and clay rich marls of variable continuity and extent. In the selected model domain (Figure 1b) the total thickness of the formation varies from > 225 m in the northwest to 175 m in the southeast. The 3 uppermost limestone sequences extend over the entire model region as homogeneous layers with a more or less uniform thickness. The clay content of the strata is in the range 5 - 15% and the physical porosity is around 3 – 5%. The Gerstenhübel Beds are a limestone sequence in the lower host rock unit with particular features. The strata thicken from west (2m) to east (about 20m). The clay and carbonate content of the Gerstenhübel Beds is variable; nevertheless, a clear internal stratification is seen. The clay-rich marls represent the “background” facies of the Effingen Beds with variable clay content (range: 20 – 40%) and porosity (range: 7 – 14%). A clear internal stratification is seen.

The quantitative description of the heterogeneous formations is derived from logging data, packer tests and geostatistical analyses obtained from borehole investigations in 5 wells in the vicinity of the selected model domain. Detailed mineralogy and porosity profiles from logging data is combined with analyses of several packer test results (Marschall et al. 2004) to derive hydraulic conductivity profiles based on the Kozeny-Carman relationship optimized for the packer test k-measurements. Hydraulic conductivities from packer tests typically range between 10^{-11} – 10^{-13} m/s. The detailed porosity and conductivity profiles are used to estimate experimental variogramms characterizing log-normal distributions that, combined with the lithostratigraphic evidence, deliver the 3D facies models. The heterogeneity of the Effingen Beds is not only characterized by the spatial variability of the different facies but also by the impact of a fracture system consisting of (1) regional fault zones, (2) major local faults, (3) minor local faults and (4) small-scale faults (Figure 1c). The fracture model is generated based on available geostatistical and hydrological information on these fault groups.

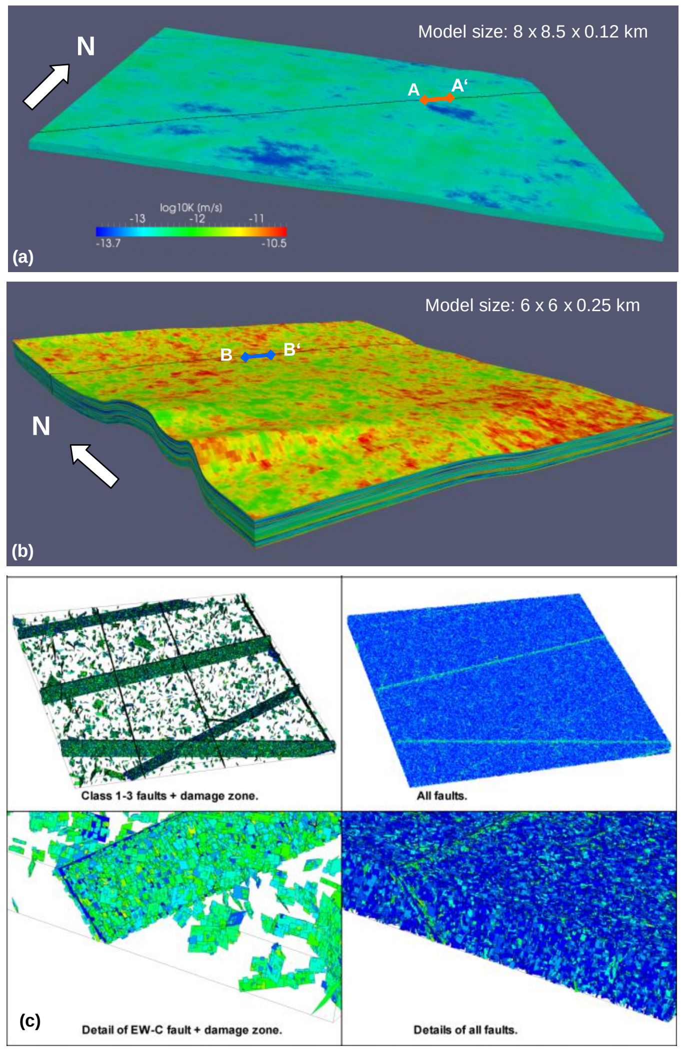

Figure 1: Stochastic models of 3D permeability distibution in the proposed host rock formations: (a) host rock model for a SF/HLW/ILW repository in the Opalinus Clay, (b) & (c) facies and fracture model, representing the host rock formation for a L/ILW repository in the Effingen Beds.

GAS TRANSPORT MODELING - FUNDAMENTALS

The numerical simulations of gas transport in the Opalinus Clay are carried out with the ITOUGH2 / TOUGH2 code family (Finsterle, 2007; Pruess et al. 1999) using the equations of state modules (EOS) for two-phase condition of hydrogen gas and water (complementary simulations: air-water). The EOS are solved isothermally, however fluid properties depend on temperature. In the simulations presented here, a constant temperature of 20 ºC is prescribed to the entire model domain, which is a good approximation as the temperature varies only a few degrees over the considered depth range. The accounted gas transfer processes are advection of gases dissolved in the liquid phase as well as advection and diffusion in a separate gas phase. In this study, diffusive mass transport in the liquid phase is neglected. Gas diffusion is described by Fick's law and advective flow is formulated with a multiphase extension of Darcy's law. Solubility of gases (hydrogen or air, respectively) in water is represented by Henry's law. Interference between the phases is represented by means of relative permeability and capillary pressure functions.

Table 1: Two-phase flow parameters (mean values) assigned to the different facies of the host rock formations Opalinus Clay and Effingen Beds

Facies	k_{harm}	ϕ	Van Genuchten Model Parameters[1]			
	$[m^2]$	[-]	P_0[Pa]	n[-]	S_{lr} [-]	S_{gr} [-]
Opalinus Clay						
Opalinus	$1{\cdot}3^{-20}$	0.09	$1.8{\cdot}10^{7}$	1.67	0.5	0.0
Effingen Beds						
Limestone layers[2]	$\sim 5{\cdot}10^{-19}$	~ 0.05	$\sim 2{\cdot}10^{6}$	1.67	0.3	0.001
Marl layers[2]	$\sim 1{\cdot}10^{-20}$	~0.08	$\sim 1.5{\cdot}10^{7}$	1.67	0.3	0.001
Gersten-hübel layer	$4{\cdot}10^{-19}$	0.05	$2.4{\cdot}10^{6}$	1.67	0.3	0.01

Two-Phase Parameter Model[1]	
van Genuchten	van Genuchten/Mualem
$P_c = P_o \cdot \left(S_{ec}^{\ n/(1-n)} - 1\right)^{1/n}$ $S_{ec} = \frac{S_l - S_{lr}}{1 - S_{lr}}$ $m = 1 - 1/n$	$k_{r,l} = S_e^{\varepsilon} \cdot \left[1 - \left(1 - S_e^{n/(1-n)}\right)^{\frac{n-1}{n}}\right]^2$ $k_{r,g} = (1 - S_e)^{\gamma}(1 - S_e^{n/(1-n)})^{2(1-1/n)}$ $S_e = \frac{S_l - S_{lr}}{1 - S_{gr} - S_{lr}}; \varepsilon = 0.5; \gamma = 0.333$

[2] The facies model of the Effingen Beds comprises a total of 7 limestone sequences and 7 marl sequences with slightly varying average values of porosity and permeability.

Capillary pressure and relative permeability are expressed in terms of two-phase parameters according to the van Genuchten-Mualem model (see Table 1). The two-phase flow parameters for the Opalinus Clay are based on analyses of laboratory tests on core samples and in-situ gas tests in boreholes (Marschall et al. 2005; Croisé et al. 2006). For the Effingen Beds, the lack of measured relative permeability relationships imposes the need to adopt information from previous studies on similar materials from a lithological viewpoint.

The spatial distribution of the capillary strength $P_{o,i}$ of a facies is generated based on average values P_o (see Table 1). We assume that P_o and permeability k_i fields are coupled via Leverett scaling (Leverett, 1941)

$$P_0 \propto \frac{1}{\sqrt{k_i}}$$

and use the k-field normalized by its harmonic mean k_{harm} to derive the P_o distribution

$$n_i = \frac{k_i}{k_{harm}} \Rightarrow P_{0,i} = \frac{P_0}{\sqrt{n_i}}$$

SF/HLW EMPALCEMENT TUNNEL

The simulations of gas release from a SF/HLW tunnel in the Opalinus Clay are carried out with 2D porosity and permeability fields, extracted from the stochastic 3D site models along the vertical cross-section A-A' in Figure 1a. In general, it is expected that gas migration might differ in 2D and 3D, mainly due to higher connectivity and available pathways in the 3D space that enhance gas flow and reduce pressure build-up in the tunnels. However, in the current context the aim is to have conservative estimates of gas pressure build-up using 2D realizations of the moderately heterogeneous Opalinus Clay. The generated parameter fields are assigned to cells of a 80x113.5 m model domain discretized with rectangular grid of 0.5x0.25 m grid size (Figure 2a). The bottom and top layer is implemented as boundary elements, corresponding to the geological units above and below the Opalinus host rock, resulting in the final 160x454 grid. The SF/HLW emplacement tunnel is included in the middle of the model domain and two half tunnels are placed at the lateral model boundaries as illustrated in Figure 2b. The tunnel cross-section is approximated with 0.5x0.25 m cells, as depicted in Figure 2b, represented by the bentonite backfill material. In order to simultaneously approximate the tunnel volume as well as the diameter of a roughly circular tunnel of a reference disposal concept, the tunnel volume in the current configuration equals that of a cylindrical tunnel with 2.325 m diameter (reference diameter in the disposal concept: 2.5 m). A steel canister is not considered in the model but a gas source term is assigned to the center cell that corresponds to bentonite. An Excavation Disturbed Zone (EDZ) is not taken into account.

The Opalinus Clay is assumed to be initially fully water saturated in the numerical simulation, while an initial gas saturation of 20% is assumed in the tunnels (emplacement saturation state of the bentonite). Initial hydrostatic pressure distribution is assigned to the entire domain (hydrostatic conditions at repository level: 6.16 MPa). The top of the model domain is considered to be at a depth of 564 m b.g. corresponding to the top of the Opalinus Clay at the location of the 2D cross section (see Figure 1a). Accordingly, hydrostatic pressure is assigned equal to 6.75 MPa and 5.63 MPa at the bottom and top boundary, respectively. No-flow boundary conditions are prescribed at the side boundaries of the model domain, providing flow process symmetry in the vicinity of the half tunnels. This approach imposes the assumption that the heterogeneous field is identical also beyond the model boundaries. Naturally, the heterogeneous field is expected to demonstrate additional variation on larger scales (i.e. see Figure 1). Nevertheless the assumption imposed here is reasonable, given the scope of this generic study to examine the impact of local-scale heterogeneity on gas transfer for subsequent transfer to larger scale models.

The gas generation rate is based on an assumed corrosion rate of the steel waste canister of $2.0 \cdot 10^{-6}$ m/a. The corresponding H_2 rate per meter emplacement tunnel is 0.0203 m^3-H_2/a/m for 77000 years. At 77000 years, the total thickness of the waste canister is assumed to have corroded.

Gas release calculations have been conducted for a range of boundary and initial conditions and for a range of two-phase flow parameters. For practical reasons, only results from the following cases are discussed in greater detail: (i) Case 1 - heterogeneous porosity and permeability distribution as presented in Figure 2a; (ii) Case 2 - homogeneous porosity (arithmetic mean of the porosity field) and homogeneous permeability (harmonic mean of the permeability field). Additional simulations have been conducted considering the arithmetic and geometric mean as well as Maxwell's effective medium theory (Neuweiler et al. 2010) for deriving effective permeability. Given that the Opalinus Clay k-field is anisotropic (ratio of correlation lengths in vertical and horizontal direction is equal to 5), the harmonic mean performed better compared to the geometric or arithmetic. Maxwell's approach, on the other hand, enhances the influence of a connected background material among *n* existing materials. It is therefore more suitable i.e. for accounting for a connected fracture field. Related remarks are provided in the discussion of gas migration in fractured Effinger members in the next section.

The results of Case 1 are shown in Figure 3 in terms of the spatial distributions of gas pressures and gas saturations at different times. The pressure front expands rather uniformly and radially around the emplacement tunnels (Figure 3a). The pressure perturbations originating from the three tunnels converge sometime before 10000 years. Similarly to the pressures, saturation distribution at different times is dominated by three radial fronts around the gas-generating tunnels that merge sometime before 10000 years (Figure 3b). Saturation barely exceeds the value of 1% locally, depending on the distribution of the host rock heterogeneous field. Gas breakthrough at the top boundary occurs sometime after 25000 years and gas remains trapped for a long time in the regions which exhibit higher permeability and lower capillary pressure.

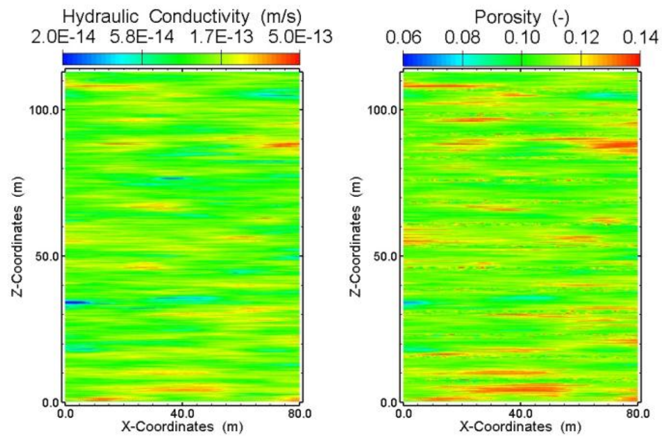

a)

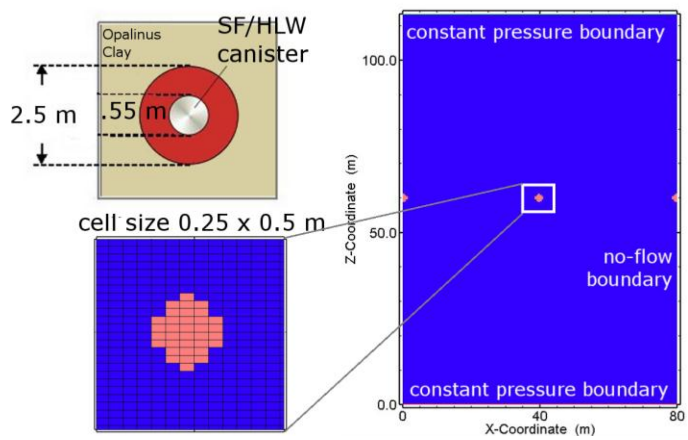

b)

Figure 2: 2D model for modeling gas release from an SF/HLW repository in the Opalinus Clay: (a) geostatistical distributions of permeability and porosity; (b) implementation of the SF/HLW emplacement tunnels.

Time-history plots generated for the pressure buildup in the different emplacement tunnels are given in Figure 4. The results of Case 2, using a harmonic average of permeability are added for comparison. The maximum pressure reached in Case 1 is 7.21 MPa and is approximately equal in all tunnels (around 1 MPa above hydrostatic pressure conditions at repository level). The pattern of pressure evolution is similar to Case 2, with pressure rapidly declining after 77000 and reaching 6.4 MPa after 100000 years. It is concluded that a homogeneous model (harmonic averaging of permeability and arithmetic averaging of porosity) is appropriate for simulating the pressure evolution in and around the underground structures. Note that the evolution of gas saturation (Figure 3b) cannot be fitted adequately with the homogeneous model.

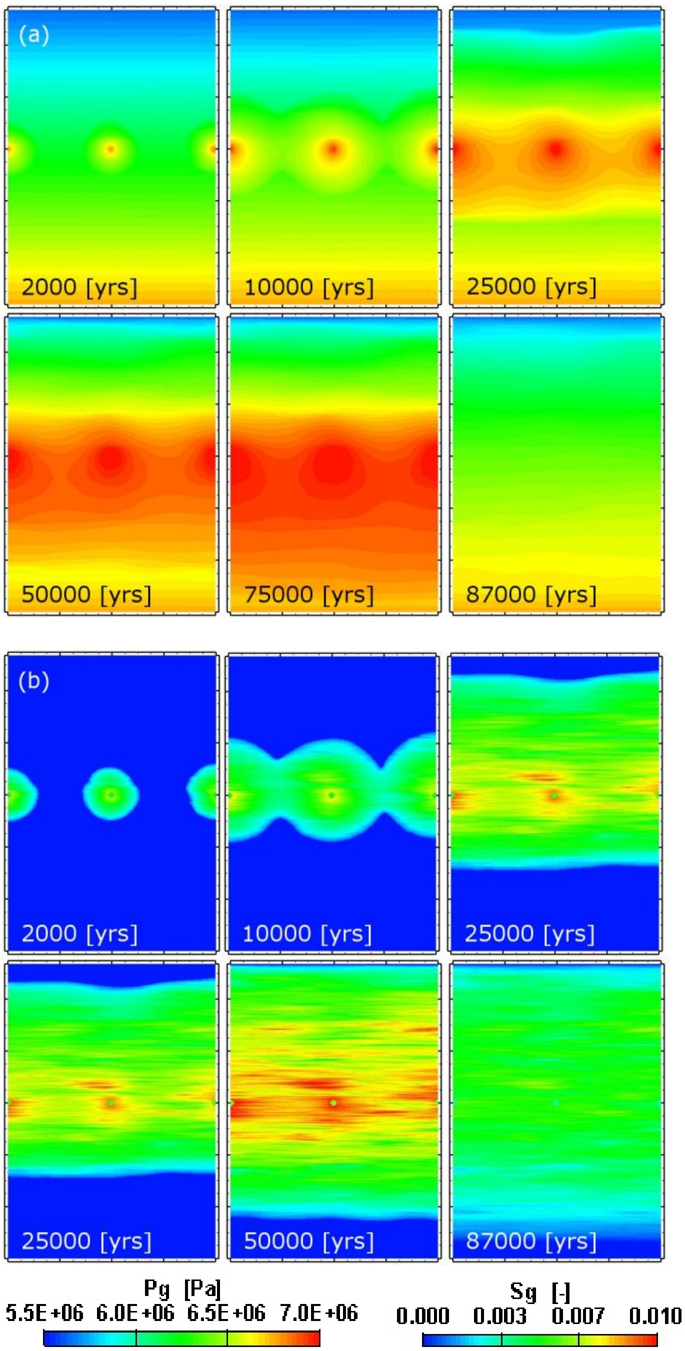

Figure 3: Gas release simulations for a SF/HLW/ILW repository in the Opalinus Clay / Case 1, showing spatial distributions of (a) gas pressures and (b) gas saturations at different times.

It must be pointed out that the simulations presented here neglect spatial variations of gas residual saturation in Opalinus Clay, assuming a uniform value of zero based on experimental evidence. Given the low gas saturation values predicted by the simulations, spatial variations of S_{gr} might have a pronounced influence on the gas migration process.

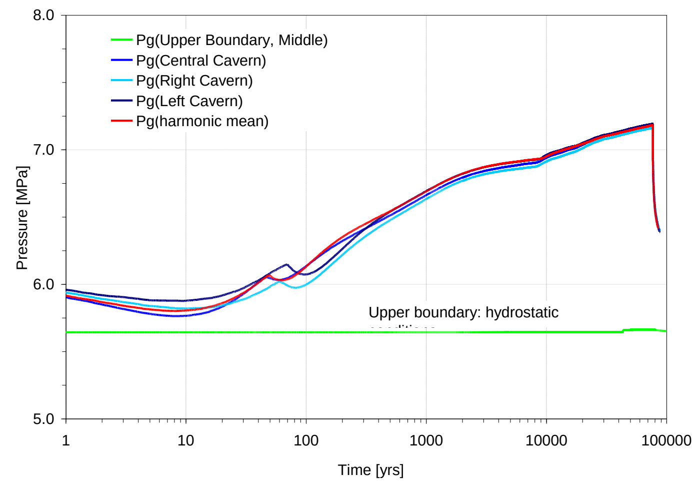

Figure 4: Time-history plots generated for the pressure buildup in the different emplacement tunnels: Comparison of Cases 1 and 2, respectively.

L/ILW EMPALCEMENT CAVERN

The simulations of gas release from a L/ILW cavern in the Effingen Beds are carried out with 2D porosity and permeability fields, extracted from the stochastic 3D site model along the vertical cross-section B-B' in Figure 1 (middle: facies model; bottom: fracture model). The extracted 2D fracture field has been corrected to account for fracture connectivity in the 3D fracture model. The generated parameter fields are assigned to a 200x251 m model domain discretized by 1x1 m cells (Figure 5). An additional bottom and top boundary layer is implemented, representing hydrostatic boundary conditions in the adjacent formation, resulting in a 200x253 m grid. Three L/ILW emplacement caverns are placed in the middle of the marl sequence as illustrated in Figure 5b. Due to process symmetry, only half of the caverns geometry is accounted for at the boundary (see also description of boundary conditions below). Caverns are approximated with 1x1 m cells as depicted in Figure 5b. Four material types are taken into account (waste packages, mortar, backfill and filling concrete). An EDZ with 1 m width is assumed. Naturally, the grid spacing used does not allow a precise representation of the L/ILW emplacement cavern and the impact of some structural components on gas migration (i.e. the exact pathway through disposal containers or the connected shotcrete lining). However, key features including main pathways through the backfill and material volumes available for gas accumulation are described adequately for the scope of these 2D calculations.

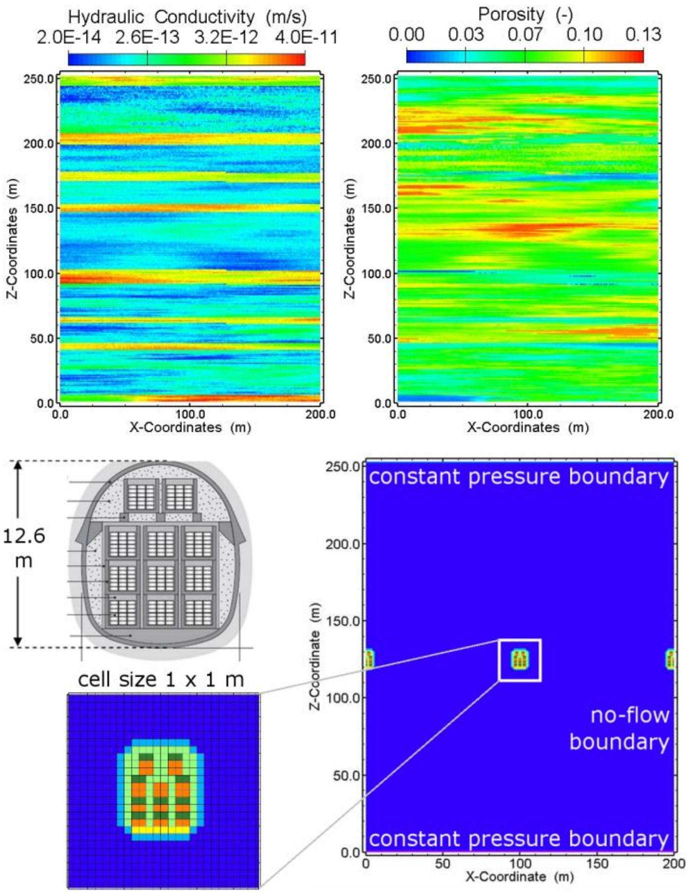

Figure 5: 2D model for modeling gas release from an L/ILW repository in the Effingen Beds: (a) geostatistical distributions of permeability and porosity; (b) implementation of the L/ILW emplacement caverns.

The Effingen Beds are assumed to be initially fully water saturated in the numerical simulation, while an initial gas saturation of 20% is prescribed inside the caverns (emplacement saturation). Initial hydrostatic pressure distribution is assigned to the entire domain. The top of the model domain is positioned at a depth of 425 m b.g. Accordingly, hydrostatic pressures are assigned equal to 4.27MPa and 6.75MPa at the top and bottom boundaries, respectively. The repository level is positioned 550 m b.g., corresponding to a hydrostatic pressure of 5.5MPa. No-flow boundary conditions are prescribed at the side boundaries of the model domain, providing flow process symmetry in the vicinity of the side caverns. Specific gas generation rates of H_2, CH_4, and CO_2 according to a preliminary L/ILW waste inventory were converted to the mass-equivalent gas generation rate of air as kg/s per m cavern length, which are assigned to the emplacement caverns.

Gas release calculations have been conducted for a range of boundary and initial conditions and for a range of the two-phase flow parameters. The following cases are discussed in greater detail: (i) Case 1 – facies model with heterogeneous porosity and permeability distribution as presented in Figure 5a; (ii) Case 2 – facies model with homogeneous porosity per facies (arithmetic mean of the porosity field) and homogeneous permeability per facies (harmonic mean of the permeability field) and (iii) Case 3 – combined facies and fracture model with heterogeneous porosity and permeability distribution. Similarly to gas migration simulations in Opalinus Clay, arithmetic, geometric means and Maxwell effective permeability per facies have been considered but will not be discussed here in great detail for practical reasons.

Additional simulations accounting for an initial operational phase of 20 years were carried out, resulting in partial desaturation and depressurization of the host rock in the vicinity of the cavern. This shifted the temporal evolution of the gas migration front and pressure build-up without influencing significantly the front morphology or maximum gas saturation and pressure values.

The results of Case 1 are shown in Figure 6a&b in terms of the spatial distributions of gas pressures and gas saturations at different times. The spatial distribution of pressure (Figure 6a) demonstrates an initial radial increase around the caverns until 10000 years followed by a uniform spread of the pressure front across the model domain until the end of the simulation. As indicated by the pressure distribution at 2000 and 10000 years, pressure buildup does not vary significantly among the three caverns.

The otherwise relatively uniform expansion of the pressure front in the host rock is in contrast to strong variations in saturation distribution due to the capillary gradients induced by the heterogeneous layered formation (Figure 6b). Indeed, saturation distribution throughout the entire simulation demonstrates a strong dependency on the facies distribution of the Effingen members. As an example, after 25000 years the marl sequence that hosts the emplacement caverns has gas saturations varying from 0.7% to 2% while the overlying limestone sequence shows a range between 10% and 18.7%. As described above, emplacement saturation in the caverns is assumed equal to 80%, a value that lies within the mobile saturation regime of the prescribed relative permeability relationships. At early times in the simulation saturation in the caverns begins to redistribute toward gravity equilibrium with water flowing in from the surrounding host rock (lower part of the emplacement caverns, t=2000 years in Figure 6b) due to the capillary pressure gradient between the partially saturated cavern materials and the host rock. As waste-generated gas accumulates in the caverns, gas pressure increases with gas eventually displacing the pore water back to the host rock (lower part of the cavern, t=10000 years in Figure 6b). In later times the flow direction is reversed once more after gas breakthrough at model boundaries and the pressure decreases accelerated by the decreasing gas generation rate. Water flow across the top boundary reversed at late time and pore water begins to flow from the host rock back into the caverns (sometime after 50000 years). However, throughout the entire simulation, gas saturation in the upper part of caverns continues to increase due to buoyancy-driven gas accumulation.

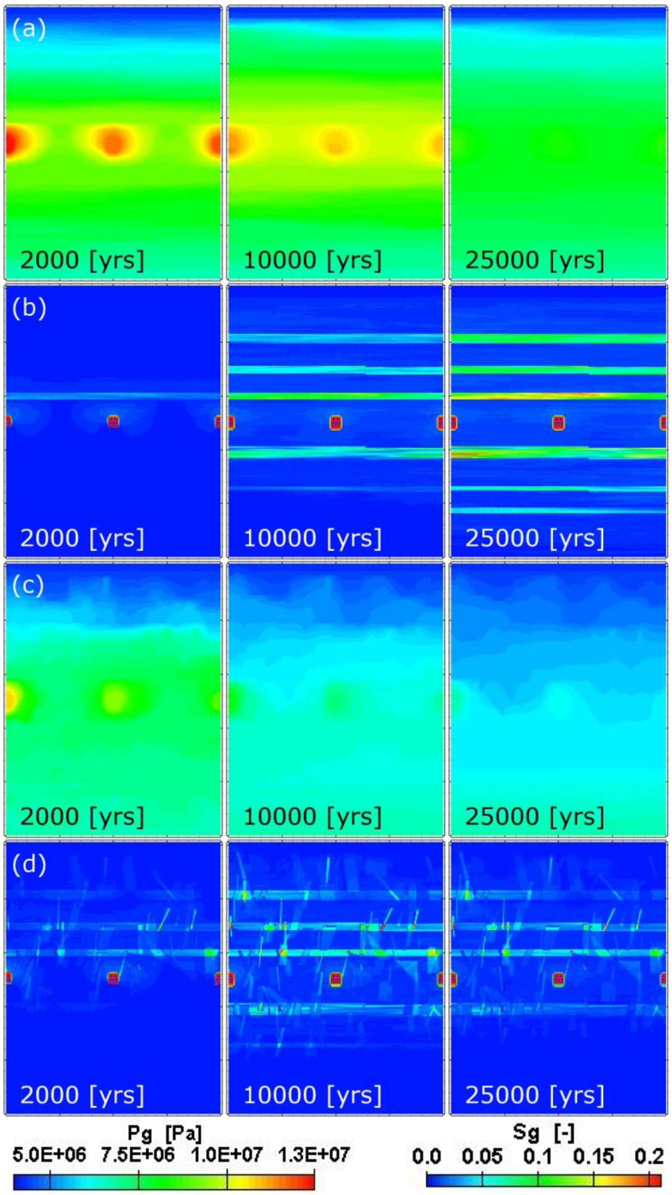

Figure 6: Gas release simulations for a L/ILW repository in the Effingen Beds: Case 1 (6a&b) and Case 3 (6c&d), showing spatial distributions of gas pressures (6a&c) and gas saturations (6b&d) at different times.

Pressure and saturation distribution from Case 3 (composite facies & fracture model) at different times is illustrated in Figures 6c&d. Compared to Case 1, the radial expansion of the pressure front is distorted as the pressure field is perturbed by strong capillary gradients introduced by the network of fractures. It is also observed that lower gas pressures prevail, already approaching quasi-stationary pressure distribution after 25000 years. The more permeable fracture network allows gas to migrate faster, reducing also the pressure build-up in the caverns. Similarly to Case 1, the left cavern demonstrates the highest gas pressure buildup.

The influence of the fracture field is pronounced in the saturation distribution (Figure 6d). Gas flows as a separate phase preferentially through the high-permeable fractures where gas saturations locally increase up to 25% after 10000 years, depending on the fracture and background host rock hydraulic properties. Similarly to Case 1, gas in the cavern initially redistributes with formation pore water infiltrating from the immediate vicinity of the cavern, then waste-generated gas displaces water back to the formation and in later times the process is reversed, with water re-occupying the lower parts of the caverns. Nevertheless, displacement of pore water out of the caverns occurs in this case but to a lesser extent, as gas preferentially migrates through the fracture network limiting the gas pressure buildup.

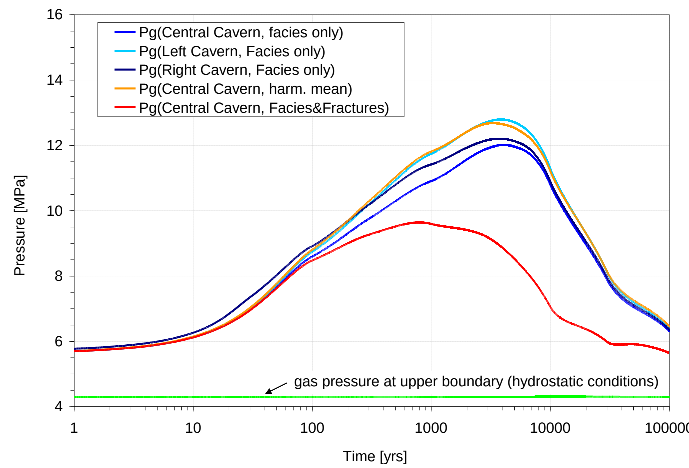

Figure 7: Time-history plots generated for the pressure buildup in the different emplacement caverns of the L/ILW repository: Comparison of Cases 1, 2 and 3, respectively.

The time-history plots of pressure buildup in the caverns are given in Figure 7. For all cases the gas pressures in the caverns start to significantly increase after 10 years with the maximum pressure values observed in the left cavern. In Case 1, the simulated buildup in the left cavern reaches a peak pressure of 12.78 MPa after 3480 years followed by a steeper decline. In the central cavern pressure reaches a maximum of 12 MPa. After approximately 10000 years pressures from the three caverns converge and decrease to 6.48 MPa after 100000 years, which is roughly 1 MPa above the corresponding hydrostatic pressure. In Case 2 the overall temporal evolution and magnitude of pressure build up are very similar to the reference Case 1; a maximum pressure of 12.74 MPa is reached after 2900 years. As in Case 1, cavern gas pressure at the end of the simulation is approximately 1 MPa higher than the hydrostatic pressure. Noticeable differences are observed in Case 3, which highlights the enhanced gas transport capacity of the composite facies&fracture model. Significantly lower gas pressures prevail in the central cavern, already approaching the hydrostatic pressure distribution after 50000 years. The more permeable fracture network allows gas to migrate faster, reducing the pressure build-up in the caverns.

Figure 8 illustrates a comparison of saturation spatial distributions from Case 1, Case 2 and a simulation using Maxwell's approach for deriving effective permeability per facies. Using harmonic permeability averages per facies produces low gas saturation values that correspond to the low-permeable materials of the facies in the detailed heterogeneous model. On the other hand, the Maxwell approach in this case considers high-permeable regions within the formation facies as connected, enhancing gas flow in the host rock. This produces higher gas saturation in the facies and lower gas pressure buildup in the cavern. Since pressure build-up in the current context is the most critical factor, harmonic averaging of individual facies was found to be more appropriate. On the other hand, the Maxwell approach can be applied for comparisons to the heterogeneous model that incorporates connected fracture fields (Case 3).

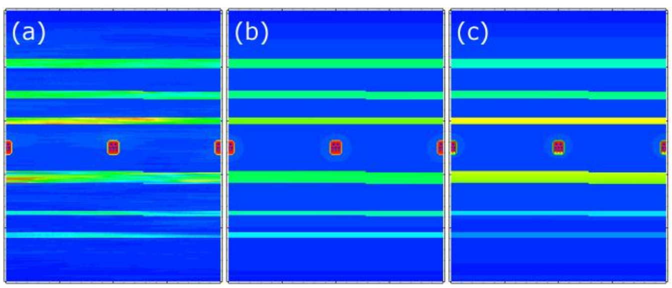

Figure 8: Gas release simulations for a L/ILW repository in the Effingen Beds: Case 1 (8a) and Case 2 (8b) compared to a simulation based on Maxwell's approach for effective permeability (8c): Spatial distributions of saturation after 25000 years.

SUMMARY AND CONCLUSIONS

In a general sense, distribution of any fluid phases in the heterogeneous host rocks is determined by the interplay between capillary, viscous and gravity forces. For a gas-water system, it is essentially expected that buoyant forces will drive gas to the surface. Whether this will be the dominant process in the system or not, depends on the viscous and capillary forces imposed by the porous medium. The saturation distributions from the simulations in the Effingen Beds indicate that the flow process is dominated by heterogeneity and especially the strong capillary contrast between limestone sequences and marl layers. The limestones have higher permeability and lower entry pressure, thus forming preferential flow paths for gas migration. Gas migration is characterized by significant lateral spreading in the limestones not only above but also below the caverns, indicating that capillarity dominates the flow regime. The effects of heterogeneity are much less pronounced in the Opalinus Clay formation, which is characterized by a moderate spatial variability of permeability represented as a single facies.

The purpose of the 2D simulations was not only to assess the effect of heterogeneity on gas migration and pressure buildup, but also to evaluate approaches for deriving effective medium properties for use in large-scale 3D models. Different averaging/upscaling techniques were compared to derive an appropriate homogeneous representation of gas transport for safety assessment calculations. The averaging procedures considered in this study indicate that harmonic averages of permeabilities for the single facies in the Opalinus Clay and for each facies of the Effingen Beds (and the corresponding capillary pressures scaling) reproduce well the cavern pressure build-up observed in the heterogeneous models. The simulations also provide a correct representation of the morphology and spreading of the gas front through the Effingen Beds, but predict lower gas saturation values in the individual facies that correspond to saturation of the low-permeable materials in each facies. An alternative approach based on Maxwell's effective medium theory puts more weight to the connectivity of high-permeable materials and thus produced higher gas flow but lower cavern pressures than those from the heterogeneous simulation. Effective medium approaches can be applied for comparisons to models that incorporate connected fracture fields.

REFERENCES

Croisé, J., Mayer, G., Marschall, P., Matray, J.-M., Tanaka, T. and Vogel, P. (2006): Gas Threshold Pressure Test Performed at the Mont Terri Rock Laboratory (Switzerland): Experimental Data and Data Analysis. Revue de l'Institut Français du Pétrole, 61 (No. 5, 2006).

Finsterle, S. (2007): iTOUGH2 User's Guide, Lawrence Berkeley National Laboratory Report LBNL-40040, Berkeley, CA.

Leverett, M.C. (1941): Capillary behavior in porous solids. Transactions of the American Institute of Mining, Metallurgical and Petroleum Engineers, 142, 152-169.

Marschall, P., Croisé, J., Schlickenrieder, L., Boisson, J.-Y., Vogel, P. and Yamamoto, S. (2004): Synthesis of hydrogeological investigations at Mont Terri site (Phases 1 to 5). Bericht des BWG, Bern, Serie Geologie 6, 7-92.

Marschall, P., Horseman, S. and Gimmi, T. (2005): Characterisation of gas transport properties of the Opalinus Clay, a potential host rock formation for radioactive waste disposal. Revue de l'Institut Français du Pétrole, 60 (No. 1&2, 2005).

Neuweiler, I., Papafotiou, A., Class, H. and Helmig, R. (2010). Estimation of effective parameters for a two-phase flow problem in non-Gaussian heterogeneous porous media, Journal of Contaminant Hydrology, doi: 10.1016/j.jconhyd.2010.08.001.

Pruess, K., Oldenburg, C. and Moridis, G. (1999): TOUGH2 user's guide, Version 2.0., Lawrence Berkeley National Laboratory Report, LBNL-43134, Berkeley, CA.